Carrier suppression in quadruple frequency modulation by cascaded optical external modulators for millimeter-wave generation

Wei Zhang (张 伟)*, Xue Feng (冯 雪), Wei Zhang (张 巍), and Xiaoming Liu (刘小明)

State Key Laboratory on Integrated Optoelectronics, Tsinghua National Laboratory for Information Science and Technology, Tsinghua University, Beijing 100084

**E-mail: zw-03@mails.tsinghua.edu.cn*

Received June 10, 2008

The optical carrier suppression in optical quadruple frequency modulation by cascaded external modulators is investigated theoretically and experimentally. Theoretical analysis demonstrates that the optical carrier suppression ratio is related with not only the initial phase difference of electrical signals applied on the two modulators, but also the optical phase shift between the two modulators. The maximum suppression ratio can be achieved when the total phase difference is equal to $n\pi + \pi/2$ $(n = 1, 2, \cdots)$, which is verified by experiments. By properly controlling the total phase shift, 40-GHz millimeter-wave is generated by using a 10-GHz radio frequency (RF) source and the modulators.

OCIS codes: 060.4080, 350.3950.

doi: 10.3788/COL20090703.0188.

In recent years, optical generation of millimeter-wave (mm-wave) is greatly interesting for many applications including millimeter radio-over-fiber system, phased-array antennas in radar systems, and so on[1−4]. For these applications, several techniques have been proposed[5−9]. Among them, optical external modulation is more attractive because of the low phase-noise and high stability[8]. Recently, a quadruple frequency modulation (QFM) scheme based on the cascaded optical external modulators was proposed[10] without the requirement of the large modulation index and additional optical filtering. In the scheme, two cascaded modulators are simultaneously driven under the same driving frequency and operating in the carrier suppressed mode, in which the carrier is suppressed while the sidebands of ±1 order are generated. Using continuous-wave (CW) monochromatic light as input carrier, the cascaded optical external modulation generates two components with a frequency interval four times of the driving frequency with the undesired original optical carrier. It has been shown that the undesired carrier can be eliminated if the phase difference of electrical driving signals of the two modulators is adjusted to $\pi/2$[10]. However, the optical phase shift introduced by the pigtail fiber between two modulators is ignored.

In this letter, we present a full analysis by considering both the electrical and optical phase shifts. It is found that the optical carrier suppression ratio is related to the differences of both the initial phase of electrical driving signals and the propagating phase shift of optical sidebands between two modulators. When the total optical phase shift difference happens on $n\pi+\pi/2$ $(n = 1, 2, \cdots)$, the optical carrier is suppressed completely and the maximum suppression ratio can be achieved. Furthermore, according to our analysis and experiment, if suppression ratio higher than 20 dB is required, the length variation of standard single mode fiber should be less than ±0.12 mm for 40-GHz mm-wave generation. Obviously, the optical phase shift should be considered in real applications for optical mm-wave generation. This conclusion is also confirmed by our further experiment, which is carried out within the electrical driving frequency of $3 - 14$ GHz. 40-GHz mm-wave is generated with a 10-GHz radio frequency (RF) source and modulators by properly controlling the phase shift. The measured phase noise and harmonic suppressed ratio are < -60 dBc/Hz @ 1 kHz and > 20 dB, respectively.

The experimental setup is shown in Fig. 1. Two cascaded intensity modulators are driven by two electrical signals from the same RF source split by a 1:1 power divider. Generally, the initial phase of each driving signals cannot keep strictly the same because the lengths of two cables from the power divider to the modulators are not identical. So the driving electrical field of each modulator should be written as $V_i(t) = V_{\mathrm{ac}} \cos(\omega_e t + \phi_i^e)$, where ω_e, V_{ac}, and ϕ_i^e $(i = 1, 2)$ are the frequency, amplitude, and initial phase, respectively. Two modulators are both biased at half-wave voltage V_π, operating at carrier suppressed mode. In the case of $V_{\mathrm{ac}} < V_\pi$, higher order sidebands

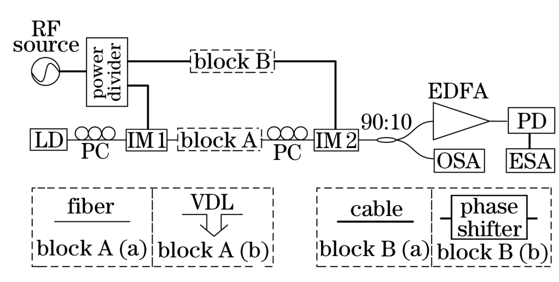

Fig. 1. Experimental setup of the mm-wave generation. Different arrangements for blocks A and B for different experiments are given at the bottom. LD: laser diode; PC: polarization controller; IM: intensity modulator; VDL: variable delay line; EDFA: erbium-doped fiber amplifier; OSA: optical spectrum analyzer; PD: photo detector; ESA: electrical spectrum analyzer.

are so weak that only ±1 order sidebands are considered[4]. When a CW light with the frequency of ω_c is launched, ±1 order sidebands at frequencies of $\omega_c \pm \omega_e$ are obtained at the output of modulator 1, with the initial phase difference of $2{\phi_1}^{e}$[10]. Subsequently, the sidebands propagate through the pigtail fiber between the modulators. The two propagating sidebands will experience different optical phase shifts according to their frequencies and fiber lengths. And the difference of the optical phase shift can be represented as $\beta_{(\omega_c-\omega_e)}L - \beta_{(\omega_c+\omega_e)}L$, where $\beta_{(\omega_c-\omega_e)}$ and $\beta_{(\omega_c+\omega_e)}$ are the propagation constants of both sidebands. By expanding to a Taylor series around the frequency ω_c, $\beta_{\omega_c\pm\omega_e}$ can be written as $\beta_{\omega_c\pm\omega_e} \approx \beta_{\omega_c} \pm \beta_1 \cdot \omega_e + \frac{1}{2}\beta_2 \cdot \omega_e^2$, then the difference of the optical phase shift can be derived as $2\beta_1\omega_e L$. So the total phase difference of ±1 order sidebands is $2\left(\phi_1^e - \beta_1\omega_e L\right)$ at the input of modulator 2. In modulator 2, both of ±1 order sidebands are modulated again, so new components at frequencies of $\omega_c - 2\omega_e$ and $\omega_c + 2\omega_e$ are generated. But at the same time, undesired optical carrier with the frequency of ω_c is also generated, which is introduced from the up/down frequency shift of $(\omega_c - \omega_e)/(\omega_c + \omega_e)$ sideband. And the phase difference can be derived as $2\left(\phi_1^e - \phi_2^e - \beta_1\omega_e L\right)$. Finally, the output from modulator 2 can be expressed as

$$\begin{aligned} E_{\text{out}} = {} & AJ_1(b_1)J_1(b_2) \\ & \times \exp\left[\mathrm{j}\left(\omega_c - 2\omega_e\right)t - \mathrm{j}\left(\beta_{(\omega_c-\omega_e)}L + \phi_1^e + \phi_2^e\right)\right] \\ & + AJ_1(b_1)J_1(b_2) \\ & \times \exp\left[\mathrm{j}\left(\omega_c + 2\omega_e\right)t - \mathrm{j}\left(\beta_{(\omega_c+\omega_e)}L - \phi_1^e - \phi_2^e\right)\right] \\ & - 2AJ_1(b_1)J_1(b_2)\exp\left(\mathrm{j}\omega_c t\right) \\ & \times \exp\left(\mathrm{j}\beta_{(\omega_c)}L\right) \cdot \cos\left(\beta_1\omega_e L - \Delta\phi^e\right), \end{aligned} \quad (1)$$

where J_1 represents the first order of first kind Bessel function, $b_i = (V_{\text{ac}}/V_{\pi i}) \cdot (\pi/2)$ $(i = 1, 2)$ is the phase modulation index for each modulator, $\Delta\phi^e = \phi_1^e - \phi_2^e$ is the applied initial phase difference of electrical driving signals. From the former two terms of Eq. (1), it can be seen that the phase shift caused by the fiber together with the electrical driving signals only affect the phase for the components at $\omega_c - 2\omega_e$ and $\omega_c + 2\omega_e$. But for the carrier at ω_c, both amplitude and phase are affected. According to the third term of Eq. (1), the intensity of component ω_c is proportional to $\cos(\beta_1\omega_e L - \Delta\phi^e)$. So it is easy to conclude that when $\beta_1\omega_e L - \Delta\phi^e$ equals $n\pi + \pi/2$, the optical carrier at ω_c can be suppressed completely and only the desired quadruple frequency components ($\omega_c - 2\omega_e$ and $\omega_c + 2\omega_e$) are reserved. This can be realized by properly adjusting $\Delta\phi^e$, L, or both of them simultaneously.

According to Eq. (1), it can be easily derived that the intensity of component ω_c is very sensitive to the pigtail fiber length L between two modulators. As an example, for standard single mode fiber ($\beta_1 = 1.5/c$, c is the light velocity in vacuum) and 10-GHz RF source, the fiber length to satisfy $\beta_1\omega_e L = \pi$ is only 10 mm. In other words, the length variation of only ∼ 5 mm can cause the optical carrier intensity to vary from maximum to minimum value.

For verifying the analysis mentioned above, some experiments are carried out. In our experimental arrangement as also shown in Fig. 1, an optical variable delay line (VDL) and an electrical phase shifter are introduced to accurately control both optical and electrical phase shifts. The tunable range and adjusting precision of the optical VDL (001-35-60-NC-SS) are ∼ 100 mm and 0.05 mm, and the operation bandwidth of the electrical phase shifter is direct current (DC) ∼ 12 GHz.

The operating wavelength of the distributed feedback laser diode (DFB-LD) is 1553.96 nm with 3.9-dBm output power. Two intensity modulators (JDSU SN-389581F) with the bandwidth of 10 GHz and $V_\pi = 5.2$ V are driven by a tunable RF source (HP 83711B) operating at 10 GHz through a 1:1 power divider (SWIEE 2968290). The driving voltage V_{ac} is about 4 V. Polarization controllers are used before each modulator to maintain the transmission loss as low as possible. The output from modulator 2 is divided to two beams by a 90:10 coupler, one is connected to an optical spectrum analyzer (OSA, ANDO AQ6317), the other is amplified by an erbium-doped fiber amplifier (EDFA) to ∼ 0 dBm and detected using a 50-GHz-bandwidth photo detector (PD, U^{2}T XPDV2120R), and then measured by an electric spectrum analyzer (ESA, Agilent E4446A).

Figure 2 shows the output optical spectra at different fiber lengths and electrical phase shifts. It can be observed that, there are only three light components. Two of them are at 1553.80 and 1554.12 nm, respectively, which are the sidebands with a wavelength interval of 0.32 nm (40 GHz). And the center one is at 1553.96 nm, corresponding to the original carrier. The intensity of carrier varies when the VDL or the electrical phase shifter is adjusted. Since it is difficult to measure the accurate pigtail fiber length and cable length, we use ΔL and $\Delta\phi$ to denote the relative path length during the adjustment of VDL and the electrical phase shift and set a reference position $\Delta L = 0$ and $\Delta\phi = 0$ when the intensity of the center component is maximum. The optical spectra with $\Delta\phi = \pi/2$, $\Delta L = 0$ and $\Delta\phi = 0$, $\Delta L = 3.3$ mm correspond to the minima of carrier intensity, both of them satisfy the condition of $\beta_1\omega_e\Delta L - \Delta\phi = n\pi + \pi/2$. Here, β_1 is equal to $2/c$ since the effective diffraction index of VDL is 2 in our experiment.

For clarity, the extinction ratio between the sidebands and carrier component versus ΔL is plotted for different $\Delta\phi$, as shown in Fig. 3, where the curves are the calculation results from Eq. (1) and the dots are the

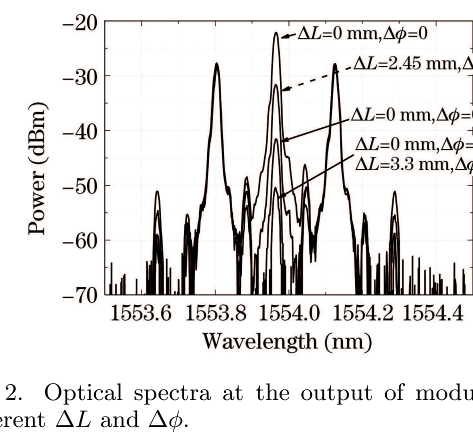

Fig. 2. Optical spectra at the output of modulator 2 with different ΔL and $\Delta\phi$.

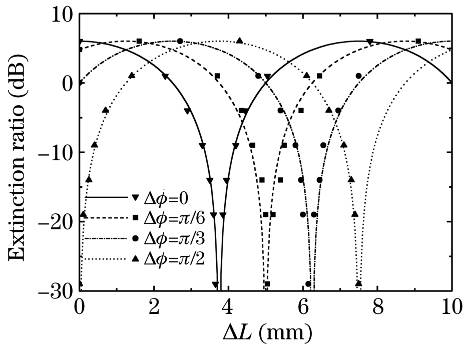

Fig. 3. Experimental (dots) and calculated (curves) extinction ratios between the sidebands and carrier component versus ΔL for different $\Delta\phi$.

experimental data. It can be observed that for different $\Delta\phi$, if the maximum extinction ratio is desired, ΔL should be adjusted to satisfy $\beta_1\omega_e\Delta L - \Delta\phi = n\pi + \pi/2$, and the length variation of standard single mode fiber should be less than ± 0.12 mm if suppression ratio higher than 20 dB is required. From Fig. 3, it can also be found that the adjusting length of VDL for a period of the radio variation is about 7.5 mm, corresponding to 10 mm of SMF length.

In addition, the adjusting length is also related to RF source, as shown in Fig. 4, where the solid line is the calculated result and the dots are the experimental data. It can be found that within the RF source frequency of $3-14$ GHz, ΔL is about $25-5$ mm to satisfy $\beta_1\omega_e\Delta L = \pi$ for both the calculated and experimental data. So the optical path is very sensitive and cannot be neglected in mm-wave generation. Furthermore, for the same pigtail fiber length, if different frequency of optical mm-wave is generated, the electrical phase shift should be adjusted.

Figure 5 shows the mm-wave after optical-electrical (O/E) conversion. It can be seen that the quadruple frequency (40 GHz) is at least 20 dB higher than the harmonics at 10, 20, and 30 GHz in the case of carrier suppressed completely. The measured phase noise is lower

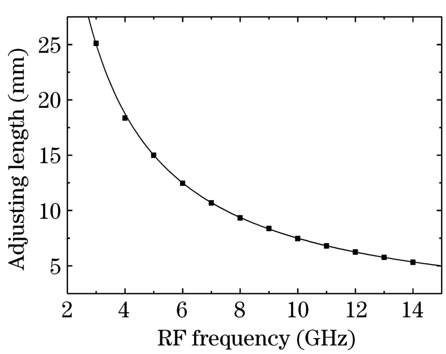

Fig. 4. Experimental (dots) and calculated (solid line) period with different frequency of RF source.

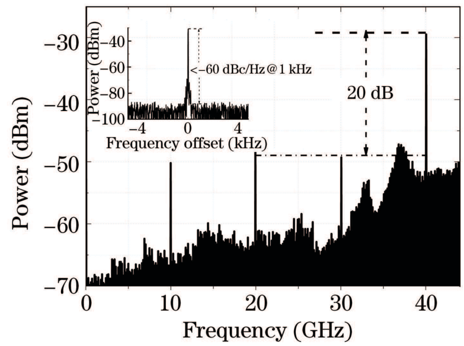

Fig. 5. Electrical spectrum of the output from PD. Inset shows the phase noise observed around 40 GHz.

than -60 dBc/Hz @ 1 kHz. The result agrees with the theory proposed in Ref. [8].

In summary, we have demonstrated a comprehensive analysis about optical carrier suppression by using optical quadruple frequency modulation with two cascaded modulators. When the difference between the initial phases of electrical driving signals and the propagating phase shift of optical sidebands between two modulators are equal to $n\pi + \pi/2$, the maximum suppression ratio can be achieved. Furthermore, from our analysis, we believe that optical fiber length is very sensitive to the intensity of optical carrier. 40-GHz mm-wave is generated with measured phase noise and harmonic suppressed ratio of < -60 dBc/Hz @ 1 kHz and > 20 dB, respectively.

This work was supported by the National "973" Program of China under Grant No. 2006CB302806.

References

1. R. P. Braun, G. Grosskopf, D. Rohde, and F. Schmidt, Electron. Lett. **32,** 626 (1996).
2. Y. Li, A. J. C. Vieira, S. M. Goldwasser, and P. R. Herczfeld, IEEE Trans. Microwave Theory Techniq. **49,** 2048 (2001).
3. J. Marti, J. L. Corral, F. Ramos, V. Polo, and J. M. Fuster, Electron. Lett. **35,** 517 (1999).
4. H. Wen, L. Chen, Y. Pi, J. Yu, and S. Wen, Chinese J. Lasers (in Chinese) **34,** 935 (2007).
5. M. Bhattacharya, B. Sarkar, and T. Chattopadhyay, IEEE Photon. Technol. Lett. **14,** 1611 (2002).
6. L. A. Johansson and A. J. Seeds, IEEE Photon. Technol. Lett. **12,** 690 (2000).
7. D. Wake, C. R. Lima, and P. A. Davies, IEEE Trans. Microwave Theory Techniq. **43,** 2270 (1995).
8. G. Qi, J. Yao, J. Seregelyi, S. Paquet, and J. C. Bélisle, Proc. SPIE **5579,** 598 (2004).
9. Q. Ye, R. Qu, and Z. Fang, Chin. Opt. Lett. **5,** 8 (2007).
10. J. Zhang, H. Chen, M. Chen, T. Wang, and S. Xie, IEEE Photon. Technol. Lett. **19,** 1057 (2007).